Materials Characterization 141 (2018) 115–119

Contents lists available at ScienceDirect

Materials Characterization

journal homepage: www.elsevier.com/locate/matchar

Effects of boron addition on the morphology of silicon phases in Al-Si casting alloys

Tengfei Gu[a], Ye Pan[a,*], Tao Lu[a], Chenlin Li[a], Jinghong Pi[b]

[a] School of Materials Science and Engineering, Jiangsu Key Laboratory of Advanced Metallic Materials, Southeast University, Nanjing 211189, China
[b] Jiangsu Key Laboratory of Advanced Structural Materials and Application Technology, Nanjing Institute of Technology, Nanjing 211167, China

ARTICLE INFO

Keywords:
Aluminium
Eutectic Si
Primary Si
Boron
Nucleation
Twins

ABSTRACT

The influence of B elements on the morphology of Si phases in Al-11Si and Al-14Si alloys has been investigated employing Optical Microscope, Scanning Electron Microscopy, Transmission Electron Microscopy and Differential Scanning Calorimetry. In Al-11Si alloy, the addition of B element not only refines the primary Al dendrites, but also reduces the length of eutectic Si plates. In Al-14Si alloys, the addition of B element promotes the nucleation temperature of primary Si phases, but shows weak influence on the nucleation temperature of eutectics. The effects of B element on the morphologies of both primary Si particle and eutectics can be attributed to the interaction between B and Si elements during the solidification process.

1. Introduction

The Al–3B master alloys are widely used as grain refiner in the fabrication of high-strength Al–Si foundry alloys, since the AlB_2 particles produced by Al-B eutectic reaction can act as the efficient nucleating sites of α-Al dendrites to refine the as-cast microstructure over a broad range of Si content (> 4 wt%) [1–5]. In addition, early works [6,7] reported that excess B addition hinders the modification of eutectic Si phase in the Sr-modified Al-Si alloys due to a mutual poisoning effect between B and Sr. On the other hand, Liu et al. [8,9] suggested that boron can react with Ca, Mg, Al and Si to precipitate Al-B-Ca-Si or Al–B–Mg–Si compounds which may act as the nuclei of primary Si grains in near eutectic Al–Si alloys. Wang et al. [10] proposed that AlB_2 particles can act as nucleates for the silicon phase through analyzing crystallographic relationship between AlB_2 and Si. However, Nogita and Dahle [3,4] compared the eutectic modification and solidification mode of Al–10Si alloys with different B additions, and their results showed that boron has no modification effect on the eutectic silicon and B-dropped samples display similar nucleation and growth characteristics of eutectic Si phases to that of unmodified alloys. Moreover, Geng et al. [11] found that boron has no significant effects on the shape factor of eutectic silicon but the mean area of eutectic Si phase is reduced when the α-Al grain size is reduced within a certain range. Dai and Liu [12] also found that boron has weak modification effect on primary silicon while it has no evident modification effect on eutectic Si phases.

Therefore, no consensus has been reached on the effect of boron addition on silicon phase (including primary Si and eutectic Si) in Al-Si foundry alloys. In this paper, the microstructures of Al-11Si and Al-14Si alloys with different B additions were investigated employing OM, SEM and TEM analysis. A special focus is on the evolution of morphology and twins of Si phases with respect to the B addition.

2. Experimental Procedure

The actual compositions of the alloys investigated in this work were obtained by Optical Emission Spectrometer (OES, MAXX LMF15) and the actual B contents were tested by Inductively Coupled Plasma-optical emission spectroscopy (ICP-OES, SPECTROBLUE) analysis. The results were in agreement with the nominal compositions as shown in Table 1.

High purity Al (99.99%) and Al-25Si (all compositions quoted in this work are in wt% unless otherwise stated) master alloys were melted in a graphite crucible to obtain Al-11Si, Al-14Si and Al-22Si alloys. Prior to adding B element in the form of Al–3B master alloys, one degassing routine was carried out with C_2Cl_6 after holding the temperature of 760 °C for 30 min. The melts were then poured into a preheated (250 ± 5 °C) ASTM: B108-2012 permanent mold. In order to ensure chemical homogenization, the melt was stirred for 30 s immediately after adding the master alloys and before casting.

Specimens for metallographic analysis were cut from a tensile test bar. The cross sections of the specimens were ground and polished using standard metallographic procedures. To analyze the microstructures, the samples were etched for 15 s or deeply etched for 2 h with 0.5 vol% HF, then observed by the optical microscope (OM,

* Corresponding author.
E-mail address: panye@seu.edu.cn (Y. Pan).

https://doi.org/10.1016/j.matchar.2018.04.050
Received 2 February 2018; Received in revised form 30 March 2018; Accepted 26 April 2018
Available online 27 April 2018
1044-5803/

Table 1
Chemical composition of alloys.

Alloys	Si (wt%)	Fe(wt%)	P (ppm)	Mg (wt%)	Cu (wt%)	B(wt%)	Al
Al-11Si	11.01	0.06	< 10	< 0.01	< 0.01	–	Balance
Al-11Si-0.05B	11.08	0.06	< 10	< 0.01	< 0.01	0.05	Balance
Al-14Si	14.49	0.08	< 10	< 0.01	< 0.01	–	Balance
Al-14Si-0.05B	14.42	0.07	< 10	< 0.01	< 0.01	0.05	Balance
Al-14Si-0.075B	14.37	0.09	< 10	< 0.01	< 0.01	0.075	Balance
Al-14Si-0.1B	14.21	0.08	< 10	< 0.01	< 0.01	0.1	Balance

Olympus BX-60 M) and scanning electron microscope (SEM, Sirion). The samples were thinned by ion-thinning device, then observed by Transmission Electron Microscopy (TEM, FEI Tecnai G2 T20). The nucleation kinetics for the experimental alloys were investigated by Differential Scanning Calorimetry (DSC, Netzsch sta449f3) experiments with constant cooling rate (8 K/min).

3. Results

3.1. Al-11Si Alloys

Fig. 1 shows the as-cast microstructures of Al-11Si and Al-11Si-0.05B alloys. Obviously, the addition of 0.05 wt% B can significantly refine the α-Al dendrites from well-developed first and secondary dendrite arms to fine and equiaxed morphology, as shown in Fig. 1a and d. The eutectic Si phases in both alloys depict plate-like morphology (the upper-right magnification SEM pictures in Fig. 1b and e, respectively), but the length of eutectic Si plate is reduced in the B-dropped alloy (Fig. 1e). TEM analysis on eutectic Si twins for both alloys (Fig. 1c and f) reveals that the density of twins increases with the addition of B element, but the growth direction of unidirectional Si twins is still $\langle 112\rangle_{Si}$ growth direction. Fig. 2 shows the DSC traces of B-free and B-dropped Al-11Si alloys, respectively, and the onset temperature of α-Al and eutectic Si phase nucleation can be clearly detected. There are two exotherm peaks for both alloys, where the exotherm peak A corresponds to the nucleation of α-Al and the peak B is associated with the nucleation of the eutectic Si. The addition of 0.05 wt% B leads to the increase of the onset temperature of α-Al nucleation from 581.9 °C to 585.9 °C, while the onset temperature of eutectic nucleation remains unchanged.

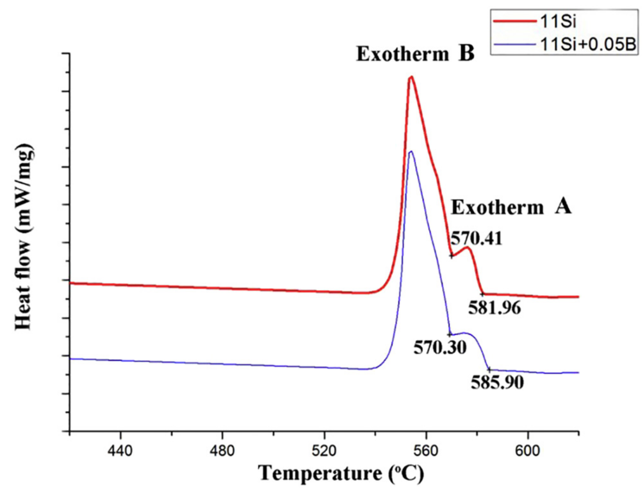

Fig. 2. Differential Scanning Calorimetry solidification exotherms of Al–11Si alloys without and with the addition of 0.05 wt%B.

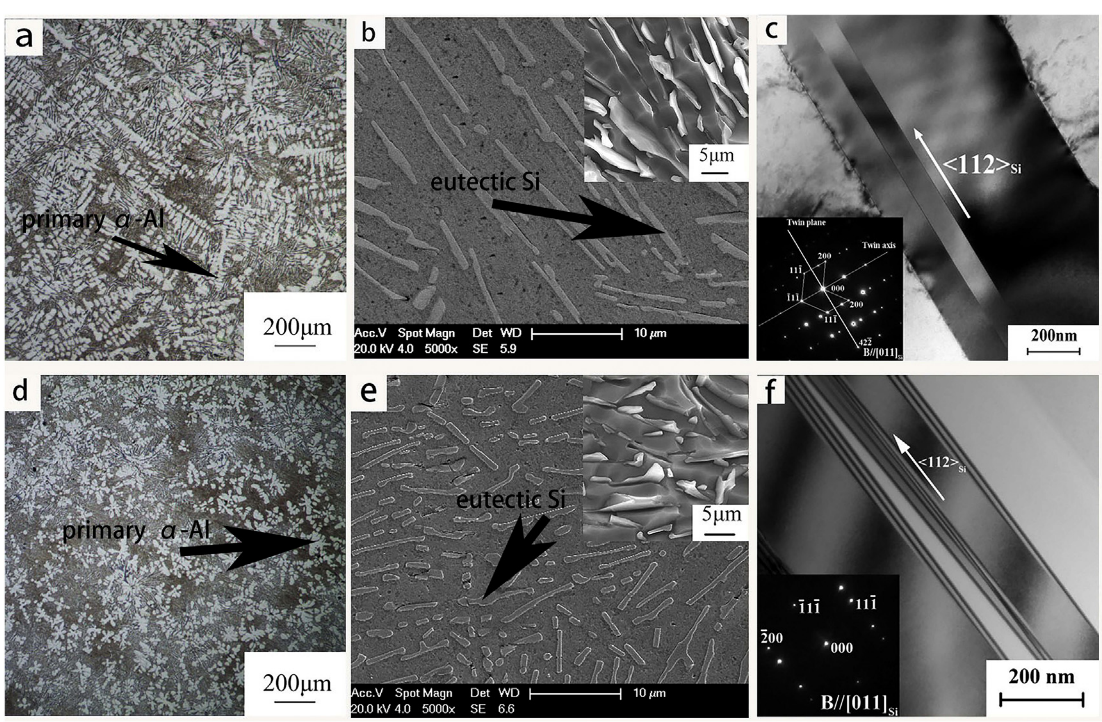

Fig. 1. The microstructures of the Al-11Si alloy (a, b, c) and the Al-11Si-0.05B alloy (d, e, f). Transmission Electron Microscopy bright field images and corresponding selected area diffraction patterns of Si particles taken from the Al-11Si alloy (c) and the Al-11Si-0.05B alloy (f). The beam is parallel to $[011]_{Si}$.